Dalton Transactions

Accepted Manuscript

ROYAL SOCIETY OF CHEMISTRY

www.rsc.org/dalton

Dalton Transactions

ARTICLE

An Aminopyrimidine-Functionalized Cage-Based Metal-Organic Framework Exhibiting Highly Selective Adsorption of C_2H_2 and CO_2 over CH_4

Received 00th January 20xx,
Accepted 00th January 20xx

DOI: 10.1039/x0xx00000x

www.rsc.org/

Jingjing Jiao,[a] Li Dou,[b] Huimin Liu,[a] Fengli Chen,[a] Dongjie Bai,[a] Yunlong Feng,[a] Shunshun Xiong,[*c] De-Li Chen[*b] and Yabing He[*a]

There has been considerable interest in adsorptive separation of C_2H_2/CH_4 and CO_2/CH_4 gas mixtures due to its industrial significance and scientific challenge. In this work, we designed and synthesized a bent diisophthalate ligand functionalized with aminopyrimidine groups, and constructed *via* a solvothermal reaction a porous copper-based framework. Single-crystal X-ray diffraction studies show the framework is a three-dimensional network containing three different types of polyhedral nanocages, which are stacked together to form two distinct types of one-dimensional channels along the crystallographical *c* axis. The compound after activation shows exceptionally high C_2H_2 and CO_2 uptakes of 211 and 120 cm^3 (STP) g^{-1} at 295 K and 1 atm, as well as impressive adsorption selectivities towards C_2H_2 and CO_2 over CH_4. High C_2H_2 and CO_2 uptake capacities as well as significant adsorption selectivities of C_2H_2 and CO_2 over CH_4 imply the potential applications in the adsorptive separation and purification of C_2H_2/CH_4 and CO_2/CH_4 gas mixtures, which have been verified by column breakthrough experiments. Several important binding sites for C_2H_2 and CO_2 in **ZJNU-54** were revealed by the quantum chemical calculations, demonstrating that the organic linkers in **ZJNU-54** form unique structures that facilitate the adsorption of C_2H_2, while the amine groups and the Lewis basic pyrimidine-ring nitrogen sites in the organic linker improve the adsorption energies for CO_2, finally leading to the increase of adsorption capacities for these two gas molecules. This work provides an efficient strategy of incorporating specific functional groups into the cage-based MOFs for generating new adsorbents for highly selective gas storage and separation.

1. Introduction

Metal-organic frameworks (MOFs),[1] which are also known as porous coordination polymers,[2] are a relatively new kind of well-ordered porous crystalline materials, which are readily assembled *via* metal coordination bonds from inorganic metal ions/clusters and organic multidentate bridging ligands. In principle, by the proper choice and combination of the inorganic and organic components, the overall structure of MOFs can be systematically tailored on the atomic level. Moreover, the pore surface properties of the MOFs can be tuned by pre-synthetical ligand functionalization approaches as well as by post-synthetic modification strategies. The chemically tuneable structure and modifiable pore environment of MOFs offer them with great advantages over traditional porous materials for myriad applications including gas storage and separation,[3] heterogeneous catalysis[4], drug delivery[5] and small molecule recognition.[6]

Among diverse porous MOFs, the cage-based MOFs have attracted great attention of chemists and materials scientists, and their research has been developed rapidly.[7] This is because polyhedral cages as supramolecular building blocks (SBBs) not only have intrinsic porosities, but also have higher connectivity compared to simple secondary building units (SBUs), which endows the whole framework with high porosity and increasing stability. Furthermore, the overall three-dimensional (3D) inter-packing of polyhedral cages usually results in special pore architectures. As a result, the cage-based MOFs frequently exhibit unique adsorption properties. A fascinating (3,24)-connected *rht*-type of MOFs constructed from dendritic hexacarboxylate ligands and dicopper paddlewheel units serve as a typical example.[8] Their structure can be viewed as the packing of three different types of polyhedral cages (cuboctahedron, truncated tetrahedron, and truncated

[a] *College of Chemistry and Life Sciences, Zhejiang Normal University, Jinhua 321004, China. E-*mail: heyabing@zjnu.cn.
[b] *Key Laboratory of the Ministry of Education for Advanced Catalysis Materials, Institute of Physical Chemistry, Zhejiang Normal University, Jinhua 321004, China. E-mail:* chendl@zjnu.cn
[c] *Institute of Nuclear Physics and Chemistry, China Academy of Engineering Physics, Mianyang, Sichuan 621900, China. E-mail: superssxiong@163.com*

Electronic Supplementary Information (ESI) available: Photograph of the crystals of ZJNU-54 (Fig. S1), PXRD (Fig. S2), TGA (Fig. S3), FTIR (Fig. S4), topology analysis (Fig. S5), BET and Langmuir plots (Fig. S6), five cycles of C_2H_2 adsorption (Fig. S7), comparison of the pure-component isotherm data with the fitted isotherms (Fig. S8), IAST calculations of mixture adsorption isotherms of **ZJNU-54a** for C_2H_2/CH_4 (50:50) and CO_2/CH_4 (50:50) at 298 K (Fig. S9). isosteric plots for C_2H_2 and CO_2 adsorption (Fig. S10), ^1H and ^{13}C NMR spectra (Fig. S11), crystal data and structure refinement for **ZJNU-54** (Table S1), Langmuir-Freundich parameters for adsorption of C_2H_2, CO_2, and CH_4 in **ZJNU-54a** (Table S2), comparison of C_2H_2 adsorption in the existing reports (Table S3), comparison of CO_2 adsorption in reported copper-diisophthalate frameworks (Table S4), CCDC 1480522. See DOI: 10.1039/x0xx00000x

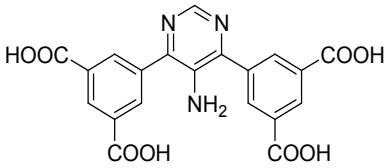

Scheme 1 The chemical structure of the organic ligand used to construct **ZJNU-54**.

octahedron), which in combination with open copper sites affords impressive performance in context of energy and environment-related gas storage for H_2, CO_2 and CH_4.[8e, 8o, 8s]

The recent advances have shown that isophthalate unit is one of well-known primary organic building units for fabricating metal-organic polyhedral cages when combined with inorganic SBUs.[9] Indeed, the integration of isophthalate units with diverse aromatic backbones led to a large number of organic linkers for the construction of a wide variety of cage-based MOFs, some of which show good to excellent gas adsorption properties.[3b, 10] If some functional sites are further anchored to aromatic backbones of the organic linkers and do not participate in coordination to metal ions, the resulting materials will be expected to exhibit enhanced gas adsorption properties. Based on the above considerations, we devised a novel angular tetracarboxylate ligand, 5,5'-(pyrimidin-5-amine-4,6-diyl) diisophthalate (H_4L, Scheme 1), which is composed of two terminal isophthalate units connected to central pyrimidine ring bearing amine group by carbon-carbon single bonds. We expect that the isophthalate unit acts as coordination sites to engender polyhedral molecule cage structure when coordination with metal ions, whereas pyridimine-5-amine serves as functional organic sites to help enhance the gas sorption properties as demonstrated in MOF literature.[8d, 8k, 8l] By employing this ligand, we successfully constructed a porous copper-based framework (which we termed **ZJNU-54**) featuring hierarchical polyhedral cage structure. As anticipated, the nitrogen donor sites are accessible within the porous framework for efficient interaction with incoming gas molecules. Gas adsorption studies shows that **ZJNU-54** after activation exhibits exceptionally high C_2H_2 and CO_2 uptakes of 211 and 120 cm^3 (STP) g^{-1} at 295 K and 1 atm as well as good C_2H_2/CH_4 and CO_2/CH_4 separation selectivities. Herein, we wish to report the synthesis, characterization and gas adsorption properties of the resulting compound.

2. Experimental

2.1 Materials and methods

Unless specifically mentioned, all reagents employed were purchased from commercial suppliers and used without further purification. 4,6-dichloropyrimidin-5-amine (purity $\geq$ 97%) was purchased from Accela ChemBio Co., Ltd.. Dimethyl 5-(pinacolboryl)isophthalate was synthesized according to our previously reported procedures.[10d] TLC analysis was performed on silica gel plates, and column chromatography was conducted over silica gel (mesh 100-200), both of which were obtained from the Qingdao Ocean Chemicals. ^{1}H NMR and ^{13}C NMR spectra were taken on Bruker AV400 or AV600 spectrophotometer at ambient temperature. Fourier transform infrared (FTIR) spectra were recorded using KBr pellet method on a Nicolet 5DX FTIR spectrometer in the range of 4000-400 cm^{-1}. Elemental analyses (C, H and N) were carried out using a Perkin-Elmer 240 CHN elemental analyser. Thermogravimetric analysis (TGA) was measured from room temperature to 1073 K on a Netzsch STA 449C instrument at a heating rate of 5 K min^{-1} under a nitrogen atmosphere. Powder X-ray diffractions (PXRD) were measured using a Philips PW3040/60 automated diffractometer with Cu-K_a radiation (λ = 1.5418 Å) with a scan speed of 2° min^{-1}. Adsorption isotherms were measured using a Micromeritics ASAP 2020 HD88 surface-area-and-porosity analyser. The gases used had the following purities (volume percentage): N_2 (99.9999%), CH_4 (99.99%), C_2H_2 (99.9%), and CO_2 (99.999%). The temperature of 77 K was maintained using a cryogenic liquid nitrogen bath, while other specified temperatures were maintained using a circulating water bath (Julabo F12).

2.2 Single-crystal X-ray diffraction

Diffraction data were collected at 150 K on a Bruker SMART APEX II CCD area-detector diffractometer equipped with graphite-monochromated Mo-K_a radiation (λ = 0.71073 Å). The structure was solved with direct methods and refined with a full-matrix least-squares technique with the SHELXTL program package. Anisotropic thermal parameters were applied to all non-hydrogen atoms. The hydrogen atoms on the organic ligands were generated geometrically. There are large solvent accessible void volumes in the crystals which are occupied by highly disordered solvent molecules. No satisfactory disorder model could be achieved, and therefore the SQUEEZE program implemented in PLATON was used to remove these electron densities.[11] The structure was further refined using the data generated. The SQUEEZE function of the program PLATON revealed a residual electron density of 1229 electrons/cell (Z = 6) in cell-remaining voids where the residual electron density was assigned to 5 DMF and 1 H_2O. Crystal data as well as details of data collection and refinements are summarized in Table S1 in the supporting information. CCDC-1480522 contains the supplementary crystallographic data for this paper. These data can be obtained free of charge from the Cambridge Crystallographic Data Centre *via* www.ccdc.cam.ac.uk/data_request/cif.

2.3 Synthesis and characterization of the organic ligand

Tetramethyl 5,5'-(pyrimidin-5-amine-4,6-diyl) diisophthalate: A mixture of 4,6-dichloropyrimidin-5-amine (0.50 g, 3.05 mmol), dimethyl (5-pinacolboryl)isophthalate (2.44 g, 7.62 mmol), $Pd(PPh_3)_4$ (0.176 g, 0.15 mmol) and Cs_2CO_3 (2.98 g, 9.15 mmol) in dioxane (80 mL) was refluxed for 48 h under nitrogen atmosphere with constant stirring. The mixture was filtered through celite and washed with hot dioxane. The organic phase was combined and concentrated under vacuum; the residue was purification by recrystallization with toluene to give the tetramethyl intermediate as a colorless solid in 27% yield (0.35 g, 0.82 mmol). ^{1}H NMR ($CDCl_3$, 400.1 MHz) δ (ppm):

8.873 (s, 1H), 8.835 (t, *J* = 1.2 Hz, 2H), 8.739 (d, *J* = 1.2 Hz, 4H), 4.103 (s, 2H), 4.022 (s, 12H); ^{13}C NMR ($CDCl_3$, 150.9 MHz) δ (ppm): 165.627, 149.915, 149.484, 137.159, 135.607, 133.710, 131.720, 131.662, 52.667.

5,5'-(pyrimidin-5-amine-4,6-diyl) di(isophthalic acid) (H_4L): To a suspension of the tetramethyl intermediate (0.35 g, 0.82 mmol) in THF (20 mL) and MeOH (20 mL) was added 6 mol L^{-1} NaOH (20 mL). The resulting mixture was heated at 318 K overnight. After removal of the solvents, the residue was dissolved in water and acidified with concentrated HCl at 273 K. The precipitation was collected by filtration, washed with water, and dried in a vacuum at 343 K to afford the target compound in almost quantitative yield. ^{1}H NMR (DMSO-d_6, 600.1 MHz) δ (ppm): 8.645 (s, 1H), 8.595 (d, *J* = 1.8 Hz, 4H), 8.566 (t, *J* = 1.8 Hz, 2H), 5.368 (s, 2H); ^{13}C NMR (DMSO-d_6, 150.9 MHz) δ (ppm): 167.297, 149.675, 147.924, 137.803, 137.541, 133.388, 133.241, 130.914; selected FTIR (KBr, cm^{-1}): 1701, 1630, 1560, 1433, 1275, 1259, 1199, 764, 687, 654, 511.

2.4 Synthesis of ZJNU-54

A mixture of H_4L (5.0 mg, 11.8 μmol), and $CuCl_2{\cdot}2H_2O$ (15.0 mg, 88.0 μmol) was dissolved in a mixed solvent of *N*,*N*-dimethyl formamide (DMF, 1.5 mL), CH_3OH (0.5 mL) and H_2O (0.1 mL). After addition 100 μL of 6 mol L^{-1} HCl, the vial was capped and heated at 353 K for 108 h. After cooling to room temperature, blue hexagon-shaped crystals were obtained. Yield: 40% based on the organic ligands. The crystals are insoluble in common organic solvents such as DMF, *N*,*N*-dimethyl acetamide (DMA), acetone, THF, dixoane, MeOH, EtOH, chloroform. Based on single-crystal X-ray structural determination, TGA and microanalysis, **ZJNU-54** can be best formulated to be $[Cu_2L(H_2O)_2]{\cdot}5DMF{\cdot}H_2O$. Selected FTIR (KBr, cm^{-1}): 1655, 1560, 1439, 1371, 1254, 1209, 1103, 775, 729, 661, 652, 486; anal. for $C_{35}H_{50}N_8O_{16}Cu_2$, calcd: C, 43.52%, H, 5.22%, N, 11.60%; found: C, 43.45%, H, 5.09%, N, 11.71%.

2.5 Fitting of pure-component isotherms

The pure component C_2H_2, CO_2 and CH_4 adsorption isotherm data measured at 278, 288 and 298 K were fitted with the singe-site Langmuir-Freundlich (SSLF) model

$$q = q_{sat}\frac{bp^v}{1+bp^v}$$

with *T*-dependent parameter *b*

$$b = b_0\exp\left(\frac{E}{RT}\right)$$

where q and q_{sat} are the amount adsorbed *per* mass of adsorbent at equilibrium pressure p, and the monolayer saturation capacity (mmol g^{-1}), b and v are Langmuir and Freundlich constants, respectively, and p is the pressure of the bulk gas at equilibrium with the adsorbed phase (kPa). The Langmuir-Freundlich parameters are provided in Table S2. Fig. S8 provides a comparison of the experimental isotherm data for C_2H_2, CO_2 and CH_4 in **ZJNU-54a** with the isotherm fits.

2.6 Column breakthrough experiments

The mixed-gas breakthrough separation experiment was carried out at 298 K and 1 atm using a lab-scale fix-bed reactor. Briefly, about 240 mg of **ZJNU-54** was packed into a stainless steel column (4 mm I.D./6.4 mm O.D. × 85 mm) with silica wool filling the void space. The MOF was activated *in situ* in the column with a vacuum pump at 298 K for 24 h followed by at 373 K for 24 h. After the column was allowed to cool to 298 K, helium was introduced to purge the adsorbent. After the flow of helium was turned off, the mixed gas (50:50 C_2H_2/CH_4 and 50:50 CO_2/CH_4) was allowed to flow into the column. The flow rate of Helium as well as the mixed gas was controlled using a mass-flow controller to be 5 mL min^{-1}. The gaseous effluent from the column was monitored using a Hiden mass spectrometer (HPR 20). Adsorbed amounts were calculated by integrating the resulting breakthrough curves by considering dead volume times, which were estimated by helium gas under the same flow rate.

2.7 Q_{st} calculations

Based on the equilibrium adsorption isotherms collected at three different temperatures, the isosteric heat of gas adsorption, Q_{st}, is determined by Clausius-Clapeyron equation, expressed as

$$Q_{st} = -R\left(\frac{\partial \ln P}{\partial(1/T)}\right)_q \quad (1)$$

where P is the pressure, T is the temperature, R is the gas constant, and q is the adsorption amount. The isostere is plotted accordingly as the $\ln P \sim 1/T$ dependence (Fig. S10), and its slope is utilized to calculate the isosteric heat of adsorption according to the equation above.

2.8 Quantum Chemical Calculations

The inclusion of van der Waals (vdW) force is important in order to accurately reproduce the weak interaction between gases and MOFs, therefore, in this study the generalized gradient approximation functional of Perdew-Burke-Ernzerhof (PBE)[12] was used to describe the exchange-correlation functional and the vdW interactions were included through use of the semi-empirical functional of Grimme (DFT-D2).[13] The details for the binding energies calculations were similar to our previous calculations for CO_2 adsorption in **ZJNU-40-45**.[10b, 10e] The unit cell of **ZJNU-54** contains 264 atoms, and the lattice parameters are a = b = 18.565 Å, c = 23.964 Å, α = β = 90º, γ = 120º. During the calculations, the lattice constants of **ZJNU-54** from experiment were fixed while all of the other atoms were completely allowed to relax, and all of the atoms were relaxed until the force on each ion was less than 0.02 eV $Å^{-1}$. All of the calculations were performed in Vienna ab initio simulation package with version of vasp.5.3.3.[14]

3 Results and Discussion

3.1 Synthesis and characterization

The organic ligand was readily synthesized by a Suzuki cross-coupling reaction between 4,6-dichloropyrimidin-5-amine and dimethyl (5-pinacol)isophthalate followed by hydrolysis and

acidification. Solvolthermal reaction of the organic ligand with $CuCl_2 \cdot 2H_2O$ in a mixed solvent of DMF, MeOH and H_2O under acidic conditions at 353 K for 108 h afforded the blue hexagon-shaped crystals which we termed **ZJNU-54** (Fig. S1). The structure was characterized by single-crystal X-ray diffraction and the bulk phase purity was confirmed by comparing the experimental and simulated PXRD patterns (Fig. S2). On the basis of the single–crystal X-ray structural determination, TGA (Fig. S3) and microanalysis, **ZJNU-54** can be formulated to be $[Cu_2L(H_2O)_2] \cdot 5DMF \cdot H_2O$. TGA showed that approximately 43.4% weight loss occurred from room temperature to 493 K, which is attributed to the release of solvent molecules and coordinated water molecules (5DMF + $3H_2O$). FTIR spectra displayed that the characteristic vibrational bands corresponding to the carboxylate group did not appear in the range of 1680–1760 cm^{-1}, indicating that the organic ligand is completely deprotonated (Fig. S4).

3.2 Structural description

Structural analysis reveals that compound crystallizes in the hexagonal space group $P6_3/mmc$. Apart from the guest molecules, the asymmetric unit consists of one fourth of the deprotonated ligand, one half of Cu(II) ion, and a half of terminal water molecule. As for the organic ligand, all the four carboxylate groups are deprotonated and coordinated to metal ions in $\mu_2{:}\eta^1\eta^1$ coordination mode (Fig. 1a). Unlike what is observed in other related MOFs constructed from bent diisophthalate ligands where there exist two conformers of the ligand,[15] the organic ligand only adopts one conformation in this compound: two outer isophthalate moieties are almost perpendicular to the inner pyrimidine ring with a dihedral angle of 89.4°. Each copper ion is penta-coordinated and bound to four equatorial carboxylate oxygen atoms and one axial oxygen atom from the terminal water resulting in the square-pyramidal coordination sphere. Two adjacent copper ions are bridged by four carboxylate groups to form a dicopper paddlewheel unit with the Cu-Cu distance being 2.656 Å, which is further connected by the organic ligands to form an extended non-interpenetrated 3D porous network occupied by solvent molecules. The most remarkable feature is that the internal NH_2 groups and pyrimidine-ring nitrogen atoms remain free and are available to bind guest molecules. Thus, **ZJNU-54** represents a rare example of a porous framework incorporating two different types of Lewis basic organic binding sites (amine groups and pyrimidine nitrogen atoms) as well as potential Lewis acidic copper sites within its pore.[16] There exist three types of polyhedral nanocages with different sizes and shapes in the network. As illustrated in Fig. 1b, the first type of cage (Cage A) with the diameter of *ca.* 10.5 Å taking into account van der Waals radii of the atoms is composed of six dicopper paddlewheels, six organic ligands and six isophthalate moieties in which six open copper sites point towards the centre of the cage and can interact with the incoming gas molecules improving the gas adsorption capacity. The second type of cages (Cage B) with the diameter of 4.3 Å consists of twelve dicopper paddlewheel units, three organic ligands and six isophthalate moieties in which the Lewis basic

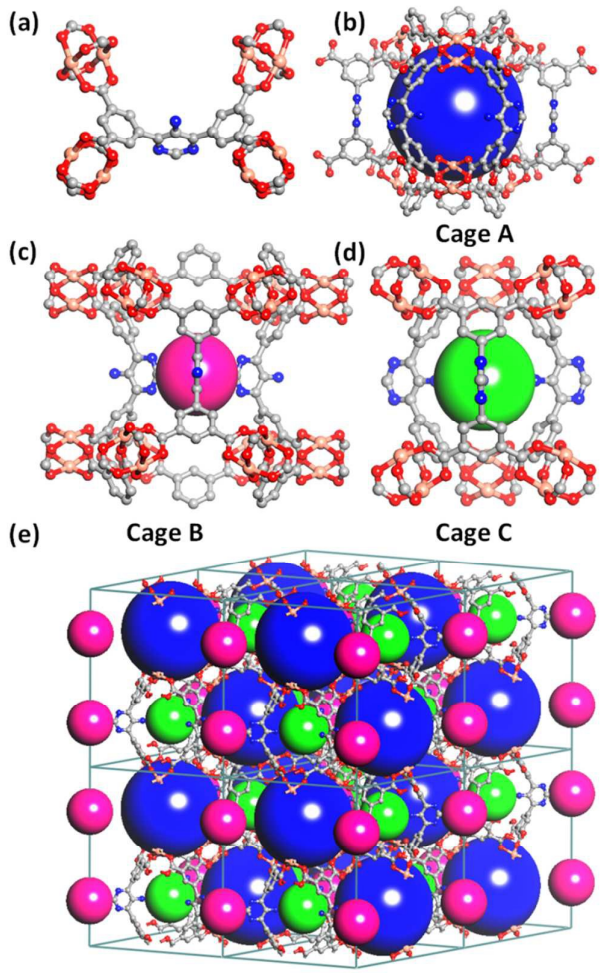

Fig. 1 Single-crystal X-ray diffraction structure of **ZJNU-54**. (a) The coordination environment of the organic linker; (b-d) three distinctly different types of polyhedral nanocages in the framework; (e) view of 3D hierarchical cage-based network. The H atoms are omitted for clarity.

pyrimidine-ring nitrogen atoms protrude into the pore centre (Fig. 1c). The third type of cages (Cage C) with the diameter of 7.8 Å is surrounded by six paddlewheel units and three organic ligands in which the uncoordinated amine groups are projected into the pore (Fig. 1d). Viewing along the crystallographical *c* axis, two distinct types of channels can be observed. One channel is formed by alternatively packing Cage A and Cage C *via* sharing three dicopper paddlewheels, while another channel is generated by packing cages B *via* sharing six dicopper paddlewheels (Fig. 1e). PLATON calculation indicates that the guest accessible volume is 64.54% of the unit cell after removal of the disordered solvent molecules and terminal water molecules (4616.7 $Å^3$ out of the 7152.97 $Å^3$ *per* unit cell volume). Topology analysis shows that the overall network is 4-connected 2-binodal network with the Schläfli symbol of $(4^2 \cdot 6^4)(4^2 \cdot 8^4)$ if the organic ligand and the dicopper paddlewheel are regarded as 4-connected nodes (Fig. S5). Alternatively, if the organic ligand is considered as having a pair of 3-coordinated branch points, the overall network is a

(3,4)-c binodal network with Schläfli symbol of $(6^2 \cdot 10^4)(6^3)_2$. It is worth noting that although the ligand bears a close resemblance to the previously reported diisophthalate ligands,[15b, 15c] the resultant MOF's structure is totally different.

3.3 Permanent porosity

To check the permanent porosity, nitrogen adsorption isotherm was measured at 77 K up to a relative pressure of 1.0. Prior to gas adsorption measurements, the as-synthesized sample was solvent-exchanged with dry acetone followed by evacuation at 373 K until the degassed rate reached 2 μmHg min^{-1} to remove any guest molecule from the sample, generating the fully desolvated **ZJNU-54a**. As demonstrated by PXRD, the framework retained intact after activation (Fig. S2). The N_2 adsorption isotherm at 77 K shows that **ZJNU-54a** displays typical Type-I adsorption behaviour with a N_2 sorption amount of 563 cm^3 (STP) g^{-1} at 1 atm (Fig. 2a), which is characteristic of microporous materials. Based on the N_2 adsorption isotherm, the Brunauer–Emmett–Teller (BET) and Langmuir surface areas are calculated to be 2134 and 2432 m^2 g^{-1}, respectively (Fig. S6), which are higher than those of **PCN-305-308** constructed from dicopper paddlewheels and a series of angular diisophthalate ligands with different functional groups.[15c] The corresponding pore volume of **ZJNU-54a** estimated from the maximum amount of N_2 adsorbed is 0.871 cm^3 g^{-1}, which is in fairly good agreement with the theoretical value of 0.847 cm^3 g^{-1} calculated from single-crystal structure with PLATON program.[11] The result also clearly indicates that the sample is well activated. Analysis by NLDFT (nonlocal density functional theory) model utilizing N_2 adsorption data at 77 K indicates that the mean pore size is predominantly around 5.9, 8.4 and 9.0 Å (Fig. 2 inset), which are close to the sizes of three cages in the framework.

3.4 C_2H_2/CH_4 and CO_2/CH_4 separation

Acetylene, the simplest unsaturated hydrocarbon with a triple bond, is an important gas playing a significant role in the people's daily life and modern chemical industry. It is widely used as gas fuel for oxy-acetylene welding and metal cutting due to high oxy-acetylene flame temperature up to 3273-4273 K. Also, acetylene is utilized as key starting material to manufacture various fine chemicals such as vinyl chloride and methyl acrylate, and electronic materials. Acetylene produced by thermal cracking of methane often contains unreacted methane. Therefore, efficient removal of CH_4 from C_2H_2 has become an important issue.[8a, 17] On the other hand, separation of CO_2 from CH_4 is also an industrially important process for natural gas purification because the coexistence of CO_2 with CH_4 not only leads to pipeline corrosion but also reduces the energy content of natural gas.[3j] The conventional cryogenic distillation is very energy-intensive for the above two separation processes. To address these issues, many alternatives are being investigated, among which physis-sorption involving porous adsorbents is emerging as promising candidate because of high efficiency and less energy consumption. Consequently, it is highly desirable to develop porous materials with high C_2H_2 and CO_2 adsorption capacities as well as high C_2H_2/CH_4 and CO_2/CH_4 separation selectivities.

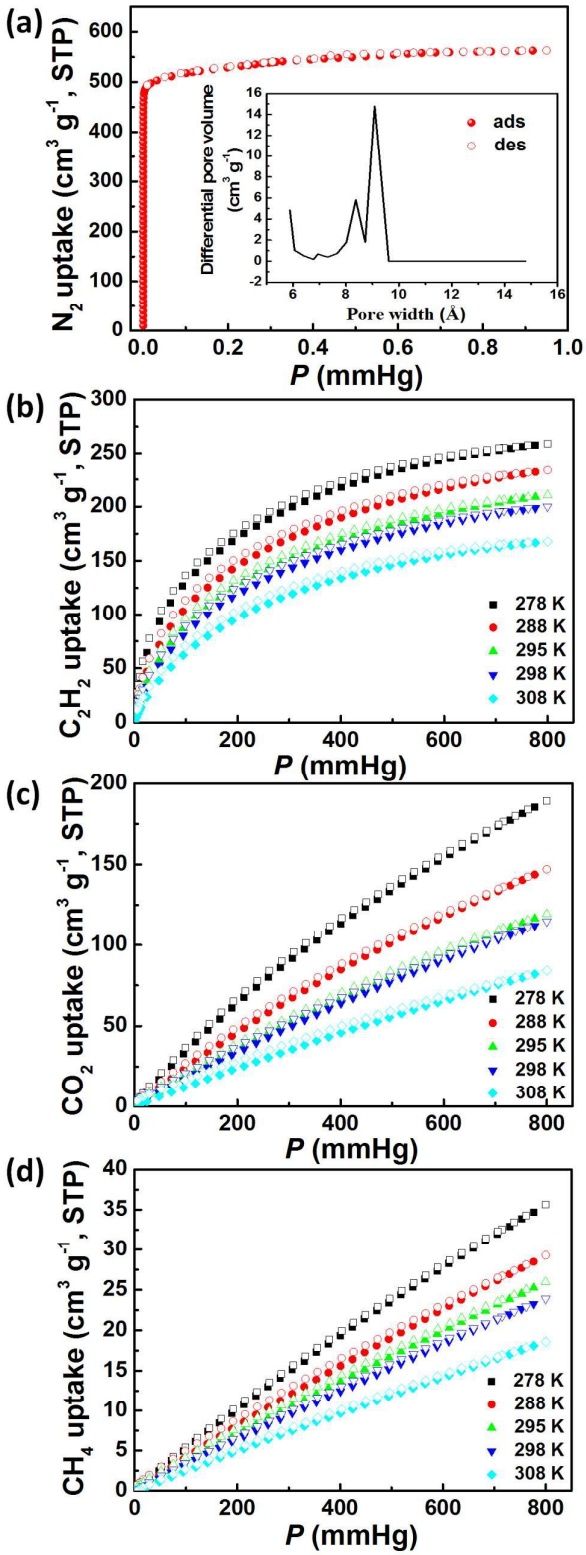

Fig. 2 N_2 adsorption-desorption isotherm of **ZJNU-54a** at 77 K. The inset shows the pore size distribution based on NLDFT model. C_2H_2 (a), CO_2 (b) and CH_4 (c) isotherms of **ZJNU-54a** at five different temperatures. Solid and open symbols represent adsorption and desorption, respectively.

In this regard, porous MOFs have attracted considerable attention and received increasing interest as suitable candidates owing to their high surface areas and designable pore structures.

The unique structure features of **ZJNU-54a** such as the rich uncoordinated nitrogen atoms and open copper sites in the pore surface, as well as hierarchical cage structure, promote us to examine its potential application on C_2H_2/CH_4 and CO_2/CH_4 separations. Accordingly, the low-pressure C_2H_2, CO_2 and CH_4 sorption properties of **ZJNU-54a** were systematically investigated by adsorption-desorption isotherms at five different temperatures of 278 K, 288 K, 295 K, 298 K and 308 K up to 1 atm, which are shown in Fig. 2b-d. No apparent hysteresis between adsorption and desorption is observed for the three gases investigated, indicating the gas adsorption on **ZJNU-54a** is reversible. It should be mentioned that essentially the same isotherms as those of the first run were obtained after four cycles, indicating that the isotherms are reproducible (Fig. S7).

Remarkably, **ZJNU-54a** displays exceptionally high sorption capacities with regard to C_2H_2 and CO_2. At 295 K, the gravimetric C_2H_2 uptake of **ZJNU-54a** increases with the increasing pressure, and reaches up to 211 cm^3 (STP) g^{-1} under 1 atm, corresponding to 31 C_2H_2 molecules adsorbed *per* formula unit (Fig. 2b). The C_2H_2 adsorption amount is among the top ranks of MOFs materials for C_2H_2 adsorption (Table S3), and is only slightly lower than that of the world-record holding MOF material **FIJ-H8** for gravimetric C_2H_2 adsorption under the similar conditions (224 cm^3 (STP) g^{-1}).[10c, 18] The C_2H_2 storage density in bulk material at 295 K and 1 atm reaches 0.186 g cm^{-3}, which is equivalent to the value of an imaginary state of C_2H_2 under 17.8 MPa at room temperature and is 88.8 times of the compression limit (0.2 MPa) for the safe storage of C_2H_2 at room temperature. When the temperature goes down from 295 K to 278 K, the amount of C_2H_2 adsorbed increased to 259 cm^3 (STP) g^{-1}. Besides, **ZJNU-54a** exhibits CO_2 uptakes of 120 and 189 cm^3 (STP) g^{-1} at 295 K and 278 K at 1 atm, respectively (Fig. 2c). The gravimetric CO_2 adsorption capacity at room temperature and 1 atm is also among the highest ever reported for copper-diisophthalate framework materials (Table S4).[10b, 10e, 15a, 15c, 19]

In sharp contrast to C_2H_2 and CO_2 adsorption, **ZJNU-54a** only adsorbs limited amounts of CH_4 (Fig. 2d). The CH_4 uptake capacities at 1 atm are 35.6 and 25.9 cm^3 (STP) g^{-1} at 278 and 295 K, respectively. Such a discrimination of adsorption capacities enables **ZJNU-54a** to be a very promising material for the selective separation of C_2H_2-CH_4 and CO_2-CH_4 gas mixtures. Ideal adsorbed solution theory (IAST) was employed to estimate the selectivity of C_2H_2 and CO_2 over CH_4 since IAST is a well-established method to predict multi-component adsorption behaviours from single-component adsorption isotherms.[20] A single-site Langmuir-Freundlich isotherm was used to fit the isotherm data at 278 K, 288 K and 298 K. The fitting results were shown in Fig. S8, and the optimally obtained fitting parameters were listed in Table S2. Fig. 3a and 3b presented the predicted IAST adsorption selectivities for equimolar C_2H_2/CH_4 and CO_2/CH_4 gas mixtures in **ZJNU-54a** as

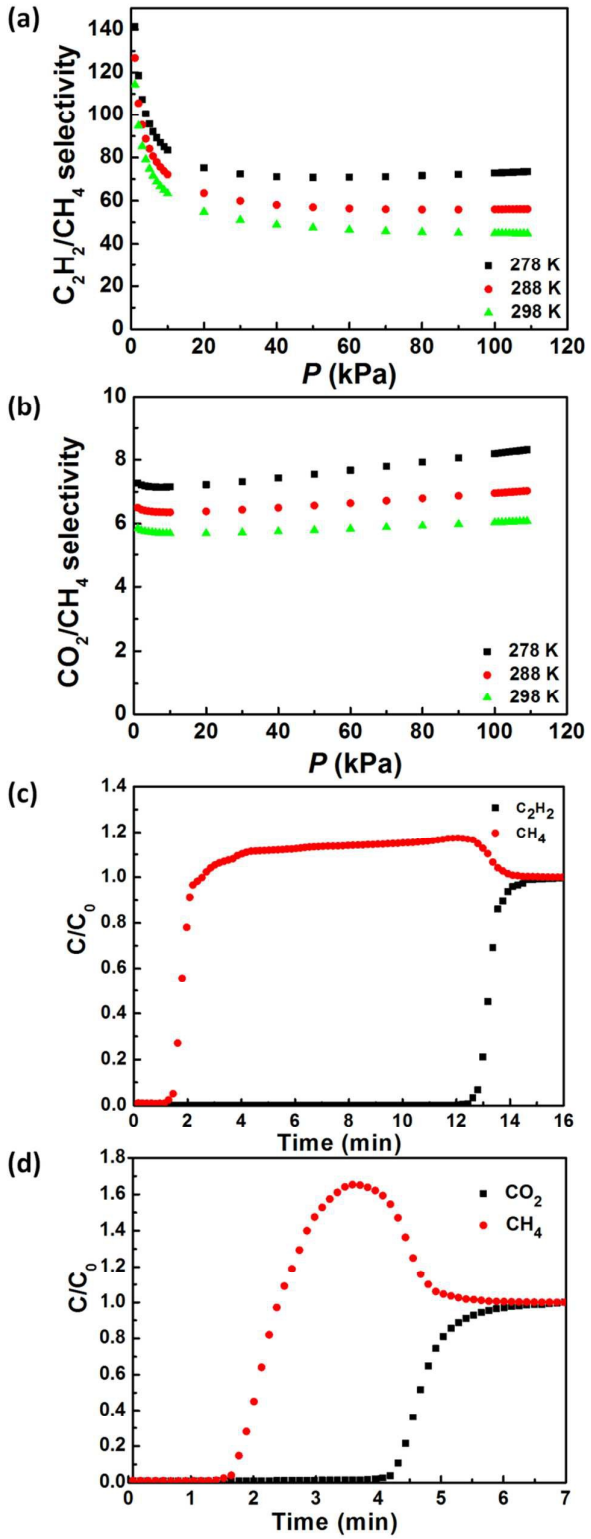

Fig. 3 IAST selectivities of (a) C_2H_2/CH_4 and (b) CO_2/CH_4 for equimolar binary gas mixtures in **ZJNU-54a**. (c) The breakthrough curves for the equimolar C_2H_2/CH_4 (c) and CO_2/CH_4 (d) gas mxitures at 298 K and 1 atm.

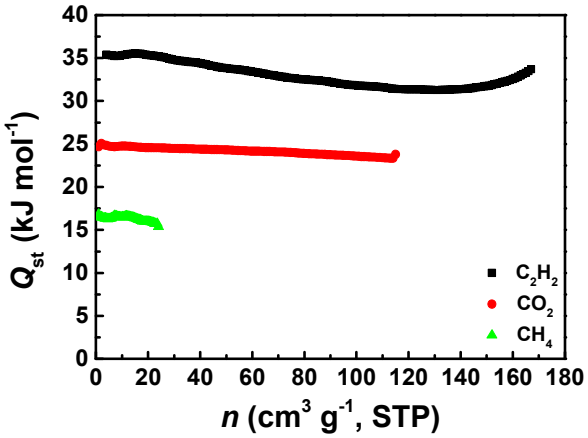

Fig. 4 The enthalpies of adsorption for C_2H_2, CO_2 and CH_4 as a function of gas loadings.

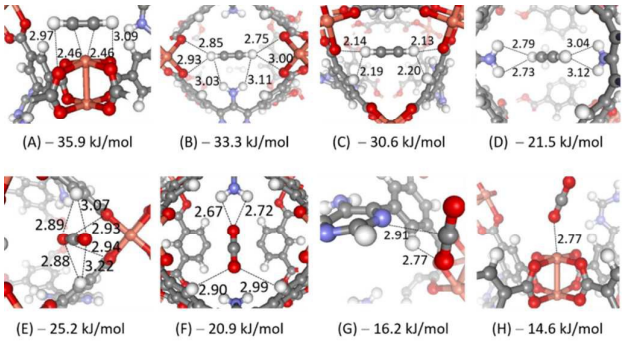

Fig. 5 Eight optimized structures representing the typical adsorption sites for (A-D) C2H2 and (E-H) CO2 in **ZJNU-54** are shown, as well as several hydrogen bond lengths and the DFT-D2 calculated binding energy for each configuration. The units for bond distance and binding energy are Å and kJ/mol, respectively. The O, H, C, Cu, and N atoms are represented with red, white, grey, brown, and blue balls, respectively.

a function of bulk pressures, respectively. The selectivities of C_2H_2 and CO_2 with respect to CH_4 are 45.0 and 6.1, respectively, at 298 K and 1 atm, which increase to 73.5 and 8.3 when the temperature is lowered down to 278 K. The CO_2/CH_4 and C_2H_2/CH_4 selectivities are impressive compared to most of the reported MOF materials. Especially, the C_2H_2/CH_4 selectivity is one of the few highest values ever reported among the porous MOF materials.[8a, 21]

Dynamic breakthrough experiments were conducted to demonstrate the separation performance of the MOF material using equimolar C_2H_2/CH_4 and CO_2/CH_4 gas mixtures. As shown in Fig. 3c and 3d, the separation of these two gas mixtures can be efficiently achieved. It is noted that a roll-up behaviour was observed for methane, which may be due to a partial substitution of the adsorbed methane on the adsorption sites by the stronger adsorptive C_2H_2 and CO_2 in the gas mixtures.[22] The dynamic C_2H_2 and CO_2 uptake capacities calculated as a result of the breakthrough time were found to be 6.16 mmol g^{-1} and 2.19 mmol g^{-1}, which are close to the IAST-predicted results (Fig. S9; 6.57 and 2.62 mmol g^{-1} for C_2H_2 and CO_2 uptakes, respectively). Based on the adsorbed amounts, the separation factors were calculated to be 39.5 and 5.2 for the equimolar C_2H_2/CH_4 and CO_2/CH_4 gas mixtures, respectively.

To figure out the reason why **ZJNU-54a** exhibits higher uptakes of C_2H_2 and CO_2 relative to CH_4, the isosteric heat of adsorption for **ZJNU-54a** is calculated using the Clausius-Clapeyron equation based on the adsorption isotherms measured at 278 K, 288 K and 298 K, and the dependence on adsorption coverage is shown in Fig. 4. With increasing coverages, the isosteric heat of adsorption does not change significantly. The heats of adsorption for C_2H_2, CO_2 and CH_4 at low coverage are 35.4, 24.7 and 16.8 kJ mol^{-1}, respectively. The Q_{st} of C_2H_2 adsorption is comparable to the value of 32.0 kJ mol^{-1} observed for **FJH-H8**.[18b] The heat of adsorption of CO_2 is comparable to those of **PCN-88** possessing CO_2 molecule traps in the framework (27.0 kJ mol^{-1})[15a], and **PCN-124** incorporating amide groups (26.3 kJ mol^{-1}).[19m] Importantly, **ZJNU-54a** possesses the higher Q_{st} values of C_2H_2 and CO_2 relative to CH_4 through the adsorption process, suggesting that C_2H_2 and CO_2 are adsorbed more strongly in **ZJNU-54a** compared with CH_4, thus responsible for highly selective separation of C_2H_2 and CO_2 over CH_4.

3.5 Quantum Chemical Calculations

Characterization of the gas adsorption/binding sites in the porous MOFs is of very importance to understand the adsorption selectivity. Currently, two effective tools to identify the gas adsorption sites within MOFs are single-crystal X-ray diffraction[23] and neutron powder diffraction.[18d, 18e, 24] Because high-resolution neutron powder diffraction equipment is not always available in common laboratory, we tried to acquire the information on the binding sites *via* single-crystal X-ray diffraction techniques at low temperature. Unfortunately, in our hands, evacuation and loading with guest molecules always generated some cracks on the crystal surface, which hinders further structural characterization. Therefore, we turned to theoretical simulations to obtain useful information.[18a, 25]

Many different initial configurations such as the open metalsite, Lewis basic N site, cage center, window sites connecting cages, and other potential important adsorption sites were built for optimization using DFT-D2 method. Based on the optimized structures, the typical adsorption sites for C_2H_2 and CO_2 in **ZJNU-54** are shown in Fig. 5, as well as their binding energies and several important bond lengths between the gas molecule and framework. The open metal site (structure A) was computed to have the largest binding energy (E_b = -35.9 kJ mol^{-1}) for C_2H_2, followed by structure B with binding energy of -33.3 kJ mol^{-1}, where the C_2H_2 molecule is well located between two dicopper paddlewheel units forming two O···H-C≡C-H···O bonding and two H (NH_2)···H (C_2H_2) hydrogen bonds. The structure C represents a favourable adsorption site of C_2H_2 at the triangular window with E_b of -30.6 kJ mol^{-1}. Comparing to the above three adsorption sites, the structure D represents an adsorption site mainly arising from the weak interaction between C_2H_2 and two amine functional groups from the organic linkers in the framework, with a much smaller binding energy of -21.5 kJ mol^{-1}, indicating the amine functional groups do not greatly improve the

adsorption of C_2H_2. Overall, the adsorption energies of structure A and B are very close to the isosteric heat of adsorption (-35.4 kJ mol^{-1}) of C_2H_2. Different from the C_2H_2 adsorption, the amine functional groups and the Lewis basic N sites play an important role in CO_2 adsorption. The structure F has a binding energy of -20.9 kJ mol^{-1}, slightly smaller than that of -25.2 kJ mol^{-1} at the window site E. The structure F in Fig. 5 shows that the several important hydrogen bonding between O (CO_2) atoms and H atoms from -NH_2 group as well as the organic linkers, with distances of 2.67, 2.72, 2.90, and 2.99 Å. In addition, the Lewis basic N site is another important adsorption site for CO_2, with binding energy of -16.2 kJ mol^{-1}, similar to the value of -14.9 kJ mol^{-1} at the open metal site. In conclusion, our vdW corrected DFT-D2 methods based calculations confirmed that the organic linkers in **ZJNU-54** form unique structures that facilitate the adsorption of C_2H_2, while the amine groups and the Lewis basic N sites in the organic linker improve the adsorption energies for CO_2, finally leading to the increase of adsorption capacities for these two gas molecules.

4. Conclusion

In conclusion, we present the design and synthesis of an aminopyrimidine-functionalized bent diisophthalate, which is used to construct a porous MOF **ZJNU-54** through coordination with $CuCl_2 \cdot 2H_2O$. In the framework, there exist three different types of cages. Moreover, open metal sites and two different types of uncoordinated nitrogen atoms are immobilized in the pore surface. **ZJNU-54** after activation shows exceptionally high C_2H_2 and CO_2 uptakes of 211 and 120 cm^3 (STP) g^{-1} at 295 K and 1 atm, which are among top ranks for C_2H_2 and CO_2 adsorption in the reported MOF materials under the similar conditions. Besides, **ZJNU-54a** exhibits impressive adsorption selectivities toward C_2H_2 and CO_2 over CH_4 at room temperature. High C_2H_2 and CO_2 uptakes as well as significant selectivities of C_2H_2 and CO_2 over CH_4 imply the potential applications of **ZJNU-54a** in the adsorptive separation and purification of C_2H_2/CH_4 and CO_2/CH_4 gas mixtures, which has also been confirmed by column breakthrough experiments. The quantum chemical calculations indicated that the organic linkers in **ZJNU-54** form unique structures that facilitate the adsorption of C_2H_2, while the amine groups and the Lewis basic N sites in the organic linker improve the adsorption energies for CO_2. This work demonstrates that incorporating specific functional organic sites, aminopyrimidine in this case, within cage-based MOFs provides an efficient strategy for the development of functional MOF materials for highly selective gas storage and separation. The work along this direction is being actively pursued.

Acknowledgements

We acknowledge the Natural Science Foundation of China (No. 21301156), the Natural Science Foundation of Zhejiang province, China (LR16B010001), and the Qianjiang talents project in Zhejiang province (ZC304015017) for financial supports. D.-L. Chen gratefully acknowledges the financial support from the National Natural Science Foundation of China (21303165).

Notes and references

1 1. O. M. Yaghi, G. Li and H. Li, *Nature*, 1995, **378**, 703-706.
2 2. S. Kitagawa, R. Kitaura and S.-i. Noro, *Angew. Chem. Int. Ed.*, 2004, **43**, 2334-2375.
3 3. (a) Y. He, W. Zhou, G. Qian and B. Chen, *Chem. Soc. Rev.*, 2014, **43**, 5657-5678; (b) Y. Yan, S. Yang, A. J. Blake and M. Schröder, *Acc. Chem. Res.*, 2014, **47**, 296-307; (c) J. A. Mason, M. Veenstra and J. R. Long, *Chem. Sci.*, 2014, **5**, 32-51; (d) Z. R. Herm, E. D. Bloch and J. R. Long, *Chem. Mater.*, 2014, **26**, 323-338; (e) J.-R. Li, J. Sculley and H.-C. Zhou, *Chem. Rev.*, 2012, **112**, 869-932; (f) M. P. Suh, H. J. Park, T. K. Prasad and D.-W. Lim, *Chem. Rev.*, 2012, **112**, 782-835; (g) T. A. Makal, J.-R. Li, W. Lu and H.-C. Zhou, *Chem. Soc. Rev.*, 2012, **41**, 7761-7779; (h) Y. He, W. Zhou, R. Krishna and B. Chen, *Chem. Commun.*, 2012, **48**, 11813-11831; (i) H. Wu, Q. Gong, D. H. Olson and J. Li, *Chem. Rev.*, 2012, **112**, 836-868; (j) K. Sumida, D. L. Rogow, J. A. Mason, T. M. McDonald, E. D. Bloch, Z. R. Herm, T.-H. Bae and J. R. Long, *Chem. Rev.*, 2012, **112**, 724-781; (k) J. Sculley, D. Yuan and H.-C. Zhou, *Energy Environ. Sci.*, 2011, **4**, 2721-2735; (l) J.-R. Li, R. J. Kuppler and H.-C. Zhou, *Chem. Soc. Rev.*, 2009, **38**, 1477-1504.
4 4. (a) M. Zhao, S. Ou and C.-D. Wu, *Acc. Chem. Res.*, 2014, **47**, 1199-1207; (b) M. Yoon, R. Srirambalaji and K. Kim, *Chem. Rev.*, 2012, **112**, 1196-1231; (c) G. Nickerl, A. Henschel, R. Grünker, K. Gedrich and S. Kaskel, *Chem. Ing. Tech.*, 2011, **83**, 90-103; (d) A. Corma, H. García and F. X. L. i. Xamena, *Chem. Rev.*, 2010, **110**, 4606-4655; (e) Y. Liu, W. Xuan and Y. Cui, *Adv. Mater.*, 2010, **22**, 4112-4135; (f) L. Ma, C. Abney and W. Lin, *Chem. Soc. Rev.*, 2009, **38**, 1248-1256; (g) J. Lee, O. K. Farha, J. Roberts, K. A. Scheidt, S. T. Nguyen and J. T. Hupp, *Chem. Soc. Rev.*, 2009, **38**, 1450-1459.
5 5. P. Horcajada, R. Gref, T. Baati, P. K. Allan, G. Maurin, P. Couvreur, G. Férey, R. E. Morris and C. Serre, *Chem. Rev.*, 2012, **112**, 1232-1268.
6 6. (a) H. Xu, H.-C. Hu, C.-S. Cao and B. Zhao, *Inorg. Chem.*, 2015, **54**, 4585-4587; (b) Z. Hu, B. J. Deibert and J. Li, *Chem. Soc. Rev.*, 2014, **43**, 5815-5840; (c) H. Wang, W. Yang and Z.-M. Sun, *Chem. Asian J.*, 2013, **8**, 982-989 ; (d) S. S. Nagarkar, B. Joarder, A. K. Chaudhari, S. Mukherjee and S. K. Ghosh, *Angew. Chem. Int. Ed.*, 2013, **52**, 2881-2885; (e) B. Chen, S. Xiang and G. Qian, *Acc. Chem. Res.*, 2010, **43**, 1115-1124.
7 7. (a) W. Lu, D. Yuan, T. A. Makal, J.-R. Li and H.-C. Zhou, *Angew. Chem. Int. Ed.*, 2012, **51**, 1580-1584; (b) U. Stoeck, S. Krause, V. Bon, I. Senkovska and S. Kaskel, *Chem. Commun.*, 2012, **48**, 10841-10843; (c) J. J. P. IV, J. A. Perman and M. J. Zaworotko, *Chem. Soc. Rev.*, 2009, **38**, 1400-1417; (d) M. J. Prakash and M. S. Lah, *Chem. Commun.*, 2009, 3326-3341.
8 8. (a) K. Liu, D. Ma, B. Li, Y. Li, K. Yao, Z. Zhang, Y. Han and Z. Shi, *J. Mater. Chem. A*, 2014, **2**, 15823-15828; (b) K. Liu, B. Li, Y. Li, X. Li, F. Yang, G. Zeng, Y. Peng, Z. Zhang, G. Li, Z. Shi, S. Feng and D. Song, *Chem. Commun.*, 2014, **50**, 5031-5033; (c) X.-J. Wang, P.-Z. Li, Y. Chen, Q. Zhang, H. Zhang, X. X. Chan, R. Ganguly, Y. Li, J. Jiang and Y. Zhao, *Sci. Rep.*, 2013, **3**, 1149; (d) Y. Yan, M. Suyetin, E. Bichoutskaia, A. J. Blake, D. R. Allan, S. A. Barnett and M. Schröder, *Chem. Sci.*, 2013, **4**, 1731-1736; (e) Y. Peng, G. Srinivas, C. E. Wilmer, I. Eryazici, R. Q. Snurr, J. T. Hupp, T. Yildirim and O. K. Farha, *Chem. Commun.*, 2013, **49**, 2992-2994; (f) C. E. Wilmer, O. K. Farha, T. Yildirim, I. Eryazici, V. Krungleviciute, A. A. Sarjeant, R. Q. Snurr and J. T. Hupp, *Energy Environ. Sci.*, 2013, **6**, 1158-1163; (g) O. K. Farha, C. E. Wilmer, I. Eryazici, B. G. Hauser, P.

A. Parilla, K. O'Neill, A. A. Sarjeant, S. T. Nguyen, R. Q. Snurr and J. T. Hupp, *J. Am. Chem. Soc.*, 2012, **134**, 9860-9863; (h) O. K. Farha, I. Eryazici, N. C. Jeong, B. G. Hauser, C. E. Wilmer, A. A. Sarjeant, R. Q. Snurr, S. T. Nguyen, A. Ö. Yazaydın and J. T. Hupp, *J. Am. Chem. Soc.*, 2012, **134**, 15016-15021; (i) B. Zheng, Z. Yang, J. Bai, Y. Li and S. Li, *Chem. Commun.*, 2012, **48**, 7025-7027; (j) R. Luebke, J. F. Eubank, A. J. Cairns, Y. Belmabkhout, L. Wojtasb and M. Eddaoudi, *Chem. Commun.*, 2012, **48**, 1455-1457; (k) B. Li, Z. Zhang, Y. Li, K. Yao, Y. Zhu, Z. Deng, F. Yang, X. Zhou, G. Li, H. Wu, N. Nijem, Y. J. Chabal, Z. Lai, Y. Han, Z. Shi, S. Feng and J. Li, *Angew. Chem. Int. Ed.*, 2012, **51**, 1412-1415; (l) B. Zheng, J. Bai, J. Duan, L. Wojtas and M. J. Zaworotko, *J. Am. Chem. Soc.*, 2011, **133**, 748-751; (m) Y. Yan, A. J. Blake, W. Lewis, S. A. Barnett, A. Dailly, N. R. Champness and M. Schröder, *Chem. Eur. J.*, 2011, **17**, 11162-11170; (n) Y. Yan, S. Yang, A. J. Blake, W. Lewis, E. Poirier, S. A. Barnett, N. R. Champness and M. Schröder, *Chem. Commun.*, 2011, **47**, 9995-9997; (o) D. Yuan, D. Zhao, D. Sun and H.-C. Zhou, *Angew. Chem. Int. Ed.*, 2010, **49**, 5357-5361; (p) O. K. Farha, A. Ö. Yazaydın, I. Eryazici, C. D. Malliakas, B. G. Hauser, M. G. Kanatzidis, S. T. Nguyen, R. Q. Snurr and J. T. Hupp, *Nature Chem.*, 2010, **2**, 944-948; (q) Y. Yan, I. Telepeni, S. Yang, X. Lin, W. Kockelmann, A. Dailly, A. J. Blake, W. Lewis, G. S. Walker, D. R. Allan, S. A. Barnett, N. R. Champness and M. Schröder, *J. Am. Chem. Soc.*, 2010, **132**, 4092-4094; (r) D. Zhao, D. Yuan, D. Sun and H.-C. Zhou, *J. Am. Chem. Soc.*, 2009, **131**, 9186-9188; (s) Y. Yan, X. Lin, S. Yang, A. J. Blake, A. Dailly, N. R. Champness, P. Hubberstey and M. Schröder, *Chem. Commun.*, 2009, 1025-1027; (t) S. Hong, M. Oh, M. Park, J. W. Yoon, J.-S. Chang and M. S. Lah, *Chem. Commun.*, 2009, 5397-5399.

9 9. Y. He, B. Li, M. O'Keeffe and B. Chen, *Chem. Soc. Rev.*, 2014, **43**, 5618-5656.

10 10. (a) C. Song, H. Liu, J. Jiao, D. Bai, W. Zhou, T. Yildirim and Y. He, *Dalton Trans.*, 2016, **45**, 7559-7562; (b) C. Song, Y. Ling, L. Jin, M. Zhang, D.-L. Chen and Y. He, *Dalton Trans.*, 2016, **45**, 190-197; (c) C. Song, J. Jiao, Q. Lin, H. Liu and Y. He, *Dalton Trans.*, 2016, **45**, 4563-4569; (d) C. Song, Y. Ling, Y. Feng, W. Zhou, T. Yildirim and Y. He, *Chem. Commun.*, 2015, **51**, 8508-8511; (e) C. Song, J. Hu, Y. Ling, Y. Feng, R. Krishna, D.-l. Chen and Y. He, *J. Mater. Chem. A*, 2015, **3**, 19417-19426.

11 11. (a) A. L. Spek, Acta Cryst., 2009, D65, 148–155; (b) A. L. Spek, Acta Cryst., 2015, C71, 9–18.

12 12. J. P. Perdew, K. Burke and M. Ernzerhof, *Phys. Rev. Lett.*, 1996, **77**, 3865.

13 13. S. Grimme, *J. Comput. Chem.*, 2006, **27**, 1787-1799.

14 14. (a) G. Kresse and J. Furthmüller, *Phys. Rev. B*, 1996, **54**, 11169-11186; (b) G. Kresse and J. Furthmüller, *Comput. Mater. Sci.*, 1996, **6**, 15-50; (c) G. Kresse, *J. Non-Cryst. Solid*, 1995, **193**, 222-229; (d) G. Kresse and J. Hafner, *Phys. Rev. B*, 1994, **49**, 14251-14264.

15 15. (a) J.-R. Li, J. Yu, W. Lu, L.-B. Sun, J. Sculley, P. B. Balbuena and H.-C. Zhou, *Nature Commun.*, 2013, **4**, 1538; (b) Z. Lu, L. Du, K. Tang and J. Bai, *Cryst. Growth Des.*, 2013, **13**, 2252-2255; (c) Y. Liu, J.-R. Li, W. M. Verdegaal, T.-F. Liu and H.-C. Zhou, *Chem. Eur. J.*, 2013, **19**, 5637-5643.

16 16. W. Yang, A. J. Davies, X. Lin, M. Suyetin, R. Matsuda, A. J. Blake, C. Wilson, W. Lewis, J. E. Parker, C. C. Tang, M. W. George, P. Hubberstey, S. Kitagawa, H. Sakamoto, E. Bichoutskaia, N. R. Champness, S. Yang and M. Schröder, *Chem. Sci.*, 2012, **3**, 2993-2999.

17 17. (a) H.-R. Fu, Y. Kang and J. Zhang, *Inorg. Chem.*, 2014, **53**, 4209-4214; (b) H. Xu, Y. He, Z. Zhang, S. Xiang, J. Cai, Y. Cui, Y. Yang, G. Qian and B. Chen, *J. Mater. Chem. A*, 2013, **1**, 77-81; (c) Z. Zhang, S. Xiang and B. Chen, *CrystEngComm*, 2011, **13**, 5983-5992; (d) E. Q. Procopio, F. Linares, C. Montoro, V. Colombo, A. Maspero, E. Barea and J. A. R. Navarro, *Angew. Chem. Int. Ed.*, 2010, **49**, 7308-7311.

18 18. (a) M. Zhang, B. Li, Y. Li, Q. Wang, W. Zhang, B. Chen, S. Li, Y. Pan, X. You and J. Bai, *Chem. Commun.*, 2016, **52**, 7241-7244; (b) J. Pang, F. Jiang, M. Wu, C. Liu, K. Su, W. Lu, D. Yuan and M. Hong, *Nat. Commun.*, 2015, **6**, 7575; (c) X. Rao, J. Cai, J. Yu, Y. He, C. Wu, W. Zhou, T. Yildirim, B. Chen and G. Qian, *Chem. Commun.*, 2013, **49**, 6719-6721; (d) S. Xiang, W. Zhou, Z. Zhang, M. A. Green, Y. Liu and B. Chen, *Angew. Chem. Int. Ed.*, 2010, **49**, 4615-4618; (e) S. Xiang, W. Zhou, J. M. Gallegos, Y. Liu and B. Chen, *J. Am. Chem. Soc.*, 2009, **131**, 12415-12419.

19 19. (a) Z. Lu, J. Bai, C. Hang, F. Meng, W. Liu, Y. Pan and X. You, *Chem. Eur. J.*, 2016, **22**, 6277-6285; (b) B. Liu, S. Yao, C. Shi, G. Li, Q. Huo and Y. Liu, *Chem. Commun.*, 2016, **52**, 3223-3226; (c) J. Cai, H. Wang, H. Wang, X. Duan, Z. Wang, Y. Cui, Y. Yang, B. Chen and G. Qian, *RSC Adv.*, 2015, **5**, 77417-77422; (d) T. K. Pal, D. De, S. Neogi, P. Pachfule, S. Senthilkumar, Q. Xu and P. K. Bharadwaj, *Chem. Eur. J.*, 2015, **21**, 19064-19070; (e) Q. Mu, H. Wang, L. Li, C. Wang, Y. Wang and X. Zhao, *Chem. Asian J.*, 2015, **10**, 1864-1869 ; (f) X. Duan, Y. He, Y. Cui, Y. Yang, R. Krishna, B. Chen and G. Qian, *RSC Adv.*, 2014, **4**, 23058-23063; (g) M. Zhang, Q. Wang, Z. Lu, H. Liu, W. Liu and J. Bai, *CrystEngComm*, 2014, **16**, 6287-6290; (h) B. Zheng, X. Lin, Z. Wang, R. Yun, Y. Fan, M. Ding, X. Hua and P. Yi, *CrystEngComm*, 2014, **16**, 9586-9589; (i) N. H. Alsmail, M. Suyetin, Y. Yan, R. Cabot, C. P. Krap, J. Lü, T. L. Easun, E. Bichoutskaia, W. Lewis, A. J. Blake and M. Schröder, *Chem. Eur. J.*, 2014, **20**, 7317-7324; (j) C. Wang, L. Li, S.-F. Tang and X. Zhao, *ACS Appl. Mater. Interfaces*, 2014, **6**, 16932-16940; (k) C. Song, Y. He, B. Li, Y. Ling, H. Wang, Y. Feng, R. Krishna and B. Chen, *Chem. Commun.*, 2014, **50**, 12105-12108; (l) Z. Wang, B. Zheng, H. Liu, X. Lin, X. Yu, P. Yi and R. Yun, *Cryst. Growth Des.*, 2013, **13**, 5001-5006; (m) J. Park, J.-R. Li, Y.-P. Chen, J. Yu, A. A. Yakovenko, Z. U. Wang, L.-B. Sun, P. B. Balbuena and H.-C. Zhou, *Chem. Commun.*, 2012, **48**; (n) X.-J. Wang, P.-Z. Li, L. Liu, Q. Zhang, P. Borah, J. D. Wong, X. X. Chan, G. Rakesh, Y. Li and Y. Zhao, *Chem. Commun.*, 2012, **48**, 10286-10288.

20 20. A. L. Myers and J. M. Prausnitz, *A.I.Ch.E.J.*, 1965, **11**, 121-127.

21 21. (a) J. Duan, W. Jin and R. Krishna, *Inorg. Chem.*, 2015, **54**, 4279-4284; (b) K. Liu, B. Li, Y. Li, X. Li, F. Yang, G. Zeng, Y. Peng, Z. Zhang, G. Li, Z. Shi, S. Feng and D. Song, *Chem. Commun.*, 2014, **50**, 5031-5033; (c) X. Duan, J. Cai, J. Yu, C. Wu, Y. Cui, Y. Yang and G. Qian, *Microporous Mesoporous Mater.*, 2013, **181**, 99-104; (d) Y. He, Z. Zhang, S. Xiang, F. R. Fronczek, R. Krishna and B. Chen, *Chem. Eur. J.*, 2012, **18**, 613-619; (e) Y. He, R. Krishna and B. Chen, *Energy Environ. Sci.*, 2012, **5**, 9107-9120

22 22. J. W. Yoon, I. T. Jang, K.-Y. Lee, Y. K. Hwang and J.-S. Chang, *Bull. Korean Chem. Soc.*, 2010, **31**, 220-223.

23 23. (a) Y. Ye, S. Xiong, X. Wu, L. Zhang, Z. Li, L. Wang, X. Ma, Q.-H. Chen, Z. Zhang and S. Xiang, *Inorg. Chem.*, 2016, **55**, 292-299; (b) X.-L. Hu, Q.-H. Gong, R.-L. Zhong, X.-L. Wang, C. Qin, H. Wang, J. Li, K.-Z. Shao and Z.-M. Su, *Chem. Eur. J.*, 2015, **21**, 7238-7244 ; (c) D. G. Samsonenko, H. Kim, Y. Sun, G.-H. Kim, H.-S. Lee and K. Kim, *Chem. Asian J.*, 2007, **2**, 484-488.

24 24. (a) S. Xiang, Y. He, Z. Zhang, H. Wu, W. Zhou, R. Krishna and B. Chen, *Nat. Commun.*, 2012, **3**, 954; (b) E. D. Bloch, W. L. Queen, R. Krishna, J. M. Zadrozny, C. M. Brown and J. R. Long, *Science*, 2012, **335**, 1606-1610.

25 25. (a) C. Song, J. Hu, Y. Ling, Y. Feng, D.-L. Chen and Y. He, *Dalton Trans.*, 2015, **44**, 14823 -14829; (b) R. B. Getman, Y.-S. Bae, C. E. Wilmer and R. Q. Snurr, *Chem. Rev.*, 2012, **112**, 703-723; (c) P. Cui, Y.-G. Ma, H.-H. Li, B. Zhao, J.-R. Li, P.

Cheng, P. B. Balbuena and H.-C. Zhou, *J. Am. Chem. Soc.*, 2012, **134**, 18892-18895.

TOC

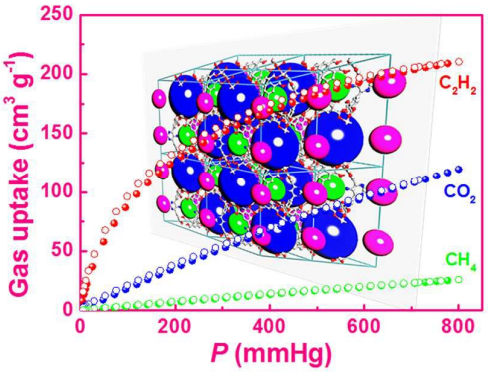

An aminopyrimidine-functionalized cage-based metal-organic framework was synthesized, exhibiting exceptionally high C_2H_2 and CO_2 uptakes as well as impressive adsorption selectivities towards C_2H_2 and CO_2 over CH_4.